

## THE DEVELOPMENT OF DATA PROCESSING TOOLS ALLOWING TO EXTRACT MORE INFORMATION ABOUT GEOMAGNETIC STORMS

ASIMOPOLOS Laurențiu, ASIMOPOLOS Adrian-Aristide, ASIMOPOLOS Natalia-Silvia

**Abstract.** In this paper, we show the Fourier and wavelet analysis of geomagnetic data recorded at the Surlari Geomagnetic Observatory (about 30 km north of Bucharest-Romania) concerning the geomagnetic storm of 28 August 2015. The Fourier analysis highlights predominant frequencies of magnetic field components. Wavelet analysis gives complete information (time, frequencies, and amplitude) of magnetic field components through variable frequency windows, that contains longer time intervals for low-frequency information, middle time intervals for medium frequency information, and short time intervals for highlight the high frequencies or details of the analysed signals. Also, the wavelet analysis allows us to decompose a geomagnetic signal into different waves. The presented analyses are only the significant ones for the geomagnetic storm period. The data for the next three days after the storm showed a mitigation of the perturbations and a transition to a quiet period from a geomagnetic point of view.

**Keywords:** Geomagnetic Storm, INTERMAGNET Network, Continuous Wavelet Transform, Discrete Wavelet Transform, 1D Fourier Transform.

**Rezumat. Dezvoltarea de instrumente de prelucrare a datelor care permit extragerea mai multor informații privind furtunile geomagnetice.** În lucrarea noastră, prezentăm analiza Fourier și wavelet a datelor geomagnetice înregistrate la Observatorul Surlari Geomagnetic (cca 30 km nord de București-România) în timpul furtunii geomagnetice din 28 august 2015. Analiza Fourier evidențiază frecvențele predominante ale componentelor câmpului magnetic. Analiza wavelet aduce informații complete (timp, frecvență, amplitudine) ale componentelor câmpului magnetic prin ferestre cu frecvență variabilă care conțin intervale de timp mai lungi pentru informații cu frecvență redusă, intervale de timp medii pentru informații de frecvență medie și intervale scurte de timp pentru evidențierea frecvențelor înalte sau a detaliilor semnalelor analizate. De asemenea, analiza wavelet permite descompunerea semnalelor geomagnetice în valori diferite. Analizele prezentate sunt doar cele semnificative pentru perioada furtunii geomagnetice. Datele pentru următoarele trei zile de după furtună au arătat atenuarea perturbațiilor și trecerea la o perioadă calmă din punct de vedere geomagnetic.

**Cuvinte cheie:** Furtuna geomagnetică, rețeaua INTERMAGNET, Transformata Wavelet Continua, Transformata Wavelet Discreta, Transformata Fourier 1D.

### INTRODUCTION

A geomagnetic storm is a temporary disturbance of the Earth's magnetosphere caused by a disturbance in space weather. Associated with solar coronal mass ejections, coronal holes, or solar flares, a geomagnetic storm is caused by a solar wind shock wave which typically strikes the Earth's magnetic field 24 to 36 hours after the event.

This only happens if the shock wave travels in a direction toward Earth. The solar wind pressure on the magnetosphere will increase or decrease depending on the Sun's activity. These solar wind pressure changes modify the electric currents in the ionosphere. Magnetic storms usually last 12 to 48 hours, but some may last for many days. The data used in this paper are acquired within the Surlari Observatory, and additional information to characterize the analysed geomagnetic storm was obtained from the sites: <http://www.intermagnet.org>, <http://www.noaa.gov>, <https://www.spaceweatherlive.com/en/archive/2015/08/28/kp>.

The analysis of geomagnetic storms is dealt with in many works from which we can recall the following: BENOIT (2012), GEBBINS & HERRERO-BERVERA (2007), ASIMOPOLOS & ASIMOPOLOS (2018), ASIMOPOLOS L. et al. (2011, 2012).

The wavelet analysis allows us to decompose a signal in different waves, called wavelets. In the case of this paper, we refer to the magnetic field components. The wavelet methodology is described in detail in the signal processing documentation, such as: CHATFIELD (1989), DAUBECHIES (1990), TORRENCE & COMPO (1998) and site: <https://www.mathworks.com/products/signal.html>. In this paper, we refer to the magnetic field components.

### DATA PROCESSING TOOLS

Wavelets allow the local analysis of magnetic field components through variable frequency windows. Windows that contain longer time intervals allow us to extract low-frequency information, average ranges of different sizes lead to extraction of medium frequency information, and very narrow windows highlight the high frequencies or details of the analysed signals. The wavelet functions describe the orthogonal bases in the  $L_2(\mathbb{R})$  space, with signal approximation properties, while the orthonormal bases in the Fourier analysis are made up of sinusoidal waves.

The estimation of geomagnetic field disturbances is similar to the standard problem of estimating a signal disturbed by signal theory.

The term noise refers to any modification that changes the periodic or quasi-periodic characteristics of the original signal.

The model of the disturbed geomagnetic field is composed of periodic oscillations plus non-periodic oscillations given by the impact of solar wind on the terrestrial magnetosphere.

The purpose of wavelet analysis is to build orthonormal bases composed of wavelets that can reconstruct the geomagnetic signals recorded in the observatories.

The wavelet algorithm was originally formulated by Goupillaud, Grossmann and Morlet in 1984 (www.mathworks.com) as a constant  $\kappa_\sigma$  subtracted from a plane wave and then localized by a Gaussian window:

$$\Psi_\sigma(t) = C_\sigma \pi^{-\frac{1}{4}} e^{-\frac{1}{2}t^2} (e^{i\alpha} - k_\sigma)$$

where:  $k_\sigma = e^{-\frac{1}{2}\sigma^2}$  is defined by the admissibility criterion and the normalization constant  $C_\sigma$  is:

$$C_\sigma = (e^{-\sigma^2} - 2e^{-\frac{3}{4}\sigma^2})^{-\frac{1}{2}}$$

Multiple resolution analysis is the core of wavelet analysis. This involves the decomposition of a signal in the subsamples at different levels of resolution.

The wavelet analysis is based on the decomposition of an approximate, constant portion, of a function  $f$  from the space  $L_2(\mathbb{R})$  in a rough approximation and a detail function.

At each level  $j$ , the approximate  $f_j$  of the given function  $f$  can be written as a sum of a gross approximation  $f_{j-1}$  located at the next approximation level and the detail function  $g_{j-1}$ , i.e.  $f_j = f_{j-1} + g_{j-1}$ . Each detail function can be written as a linear combination of mother wavelet functions:

$$\psi_{j,k}(x) = 2^{\frac{j}{2}} \psi(2^j x - k)$$

where  $j$  is the index of dilatation and  $k$  is the index of translation,  $j, k \in \mathbb{Z}$ . When the index  $j$  gets higher, the approximate approximations become finer. For each level of resolution we have a basic function area  $(\psi_{j,k})$ ,  $j, k \in \mathbb{Z}$ . Therefore, we will work with multiple areas at different resolutions (multiresolution). In Fig. 1 are division of time-frequency plan (time on x-axis and frequency on y-axis) for wavelet analysis, Fourier transform and Fourier transform in the short term (LIU, 2010, www.mathworks.com):

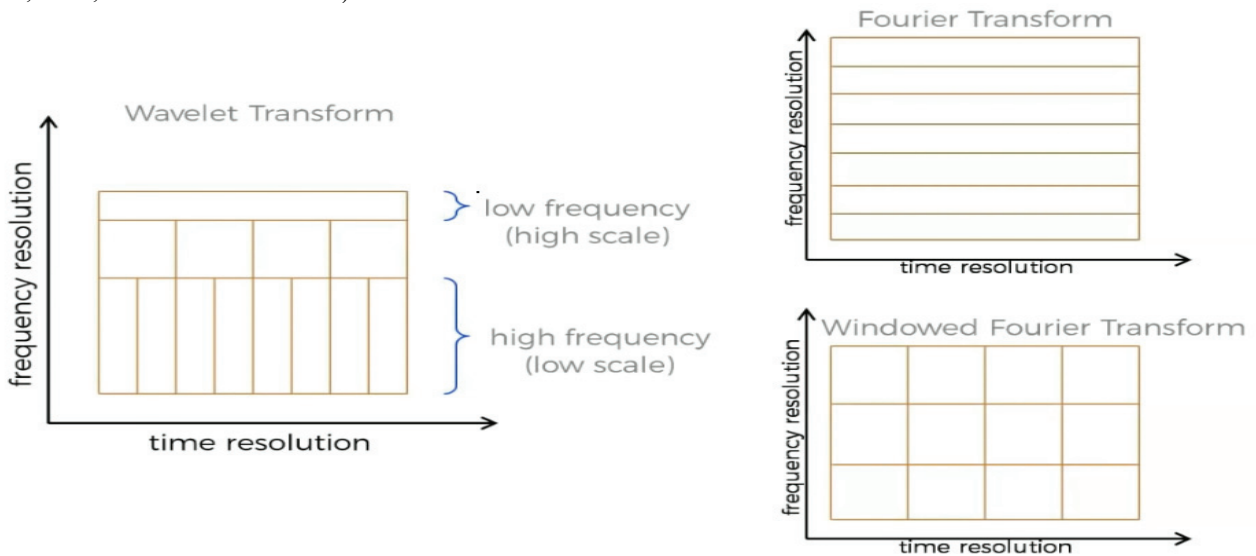


Figure 1. Different time-frequency tile allocation of the three transforms: wavelet transform, Fourier transform, Windowed Fourier Transform (STFT).

The wavelet function is designed to strike a balance between the time domain (finite length) and the frequency domain (finite bandwidth). As we dilate and translate the mother wavelet, we can see very low frequency components at the large  $s$  while very high frequency component can be located precisely at the small  $s$ .

The transition from STFT to wavelet was done by replacing a fixed-length analysis window, regardless of the frequency of the studied signal, with a set of variable duration analysis windows, so that at low frequencies we use long duration, and at high frequencies we use small durations.

To make the Wavelet Continue Transform (CWT), a real or complex signal must satisfy the following two conditions:

$$\int_{-\infty}^{\infty} \psi(t) dt = 0 \quad , \quad \int_{-\infty}^{\infty} |\psi(t)|^2 dt < \infty$$

The first property, according to which the signal has a mean null value, suggests a possible oscillating aspect, while the second property, referring to the finite energy value, indicates that the signal concentrates most of the energy within a finite range of time.

The two conditions, together with a so-called admissibility condition (required to define the transformed wavelet inverse), are sufficient for a signal to "qualify" as a wavelet signal. In the literature, numerous such signals have been proposed, some of them with finite (thus compact support) and others with infinite duration, but with concentrated energy within a finite timeframe. Fig. 2 shows examples of wavelet signals (www.mathworks.com) and Fig. 3 shows the different bases for transforms.

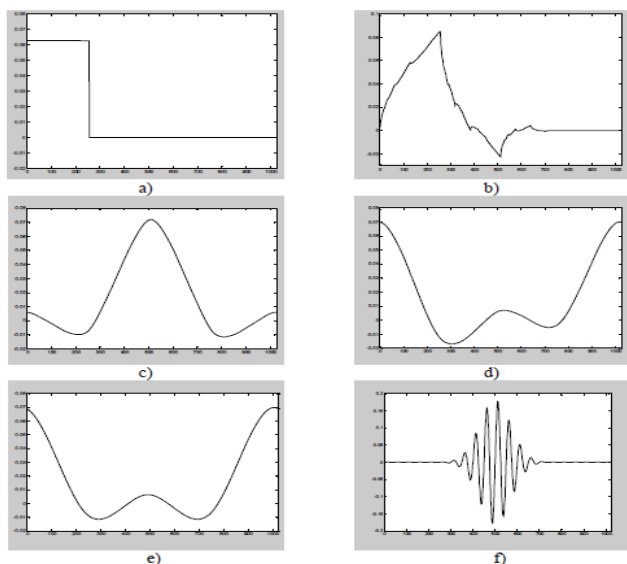


Figure 2. Examples of wavelet signals. a) Haar; b) Daubechies; c) Coiflet; d) Symmlet; e) Battle-Lemarie; f) Morlet (www.mathworks.com).

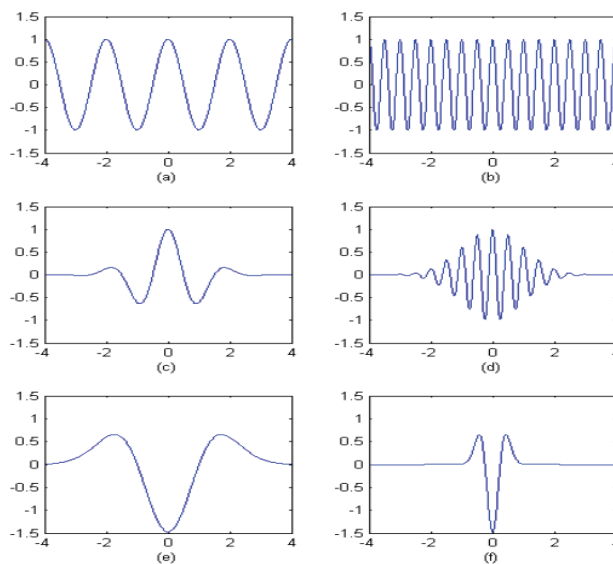


Figure 3. Different bases for transforms. (a) Real part of the basis for Fourier transform,  $\exp(j\pi t)$ . (b) Basis for different frequency,  $\exp(j4\pi t)$ . (c) Basis for STFT, using Gaussian window of  $\sigma = 1$ . It is:  $\exp(-t^2/2) \exp(j\pi t)$ . (d) Basis for different frequency,  $\exp(-t^2/2) \exp(j4\pi t)$ . (e) Mexican-hat mother wavelet function and (f)  $s = 4$ . (www.mathworks.com).

In both the Fourier Transform and the Wavelet Transformation, the transformation evaluation involves the calculation of a scalar product between the analysed signal and a set of signals that form a particular base in the vector space of the finite energy signals. The Fourier representation uses an orthogonal vector basis, whereas in the case of wavelet there is the possibility to use also bases consisting of independent linear non-orthogonal vectors. Unlike the Fourier transform, which depends only on a single parameter, wavelet transform type depends on 2 parameters (a and b). As a result, the graphical representation of the spectrum is different. Examples in this regard are illustrated, from www.mathworks.com, in Figs. 4-5.

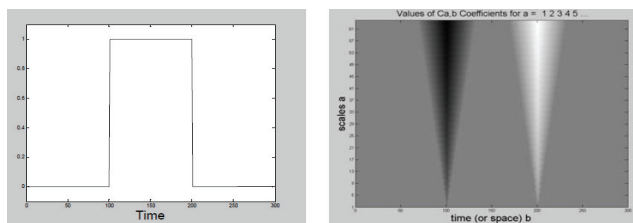


Figure 4. Graphical representation of the CWT transformation corresponding to elementary signals (www.mathworks.com).

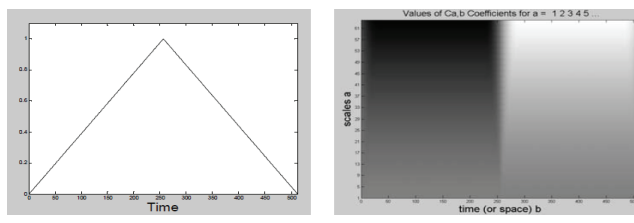


Figure 5. Graphical representation of the CWT transformation (www.mathworks.com).

### EXPERIMENTAL RESULTS OF WAVELET ANALYSIS

In our example, we used the data recorded at the Surlari Geomagnetic Observatory at a frequency of 2Hz to identify correlations occurring between the high frequency oscillations of the geomagnetic field components over day, 2015, August 28, 00:00:00 to 24:00:00). We used in the Fourier and wavelet analysis 172800 samples at 2 Hz sampling rates, where we can view the predominant frequencies for each point and can be distinguished range of frequencies.

We used for the Fourier analysis the MATLAB with the code presented in ANNEX. Also, for the wavelet analysis we used function Daubechies db1, at level 5, the same wavelet as Haar, with the code presented in ANNEX.

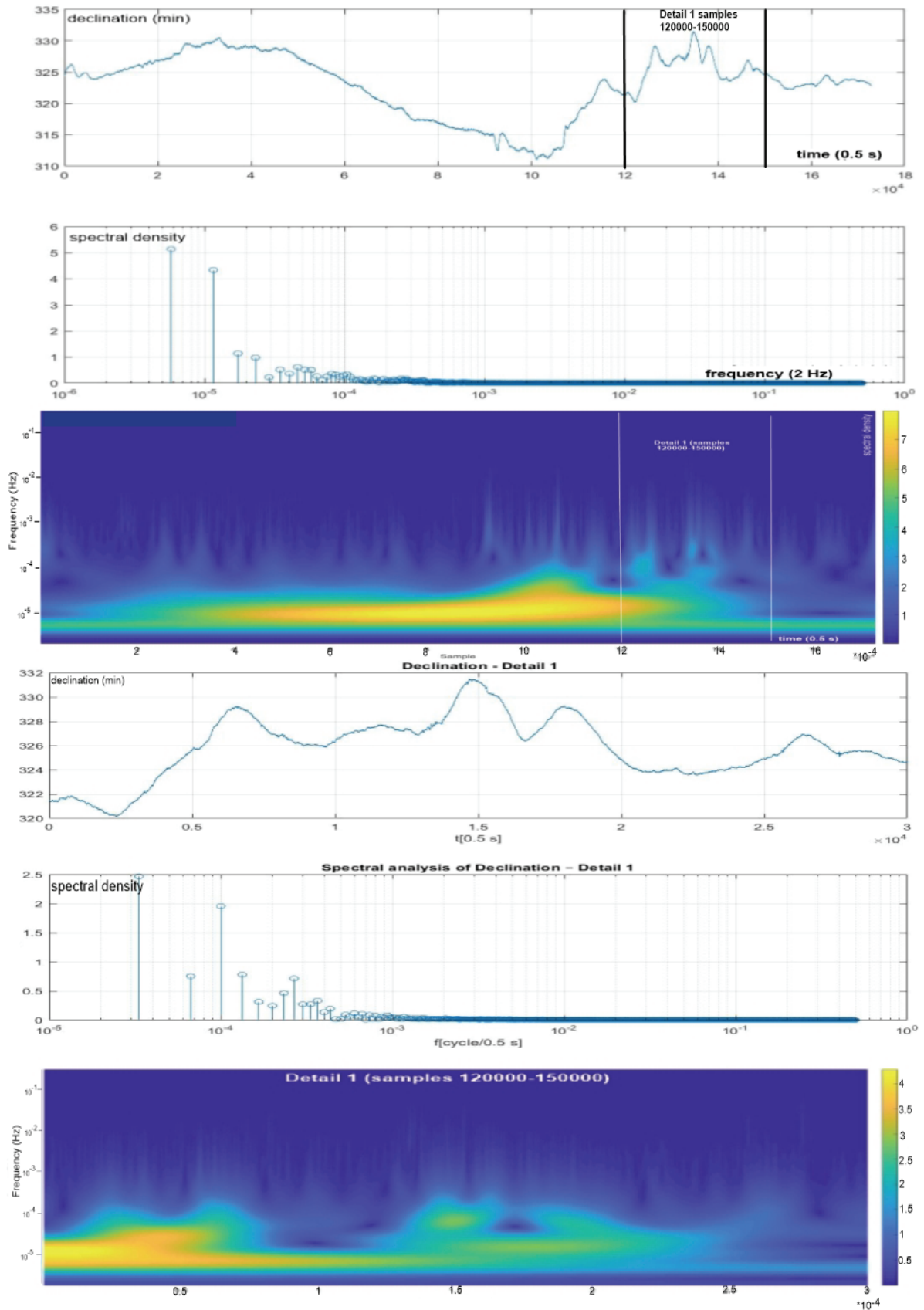


Figure 6. Time series, spectral analysis and wavelet analysis of declination. From top to bottom the images have the following meaning: In the first three images we have the time series, Fourier analysis and wavelet analysis for all days of 2015, August 28, 00:00:00 to 24:00:00. In the last three images we have the time series, Fourier analysis and wavelet analysis for Detail 1 – interval 120000-150000 samples - a range of 4 hours and 10 minutes.

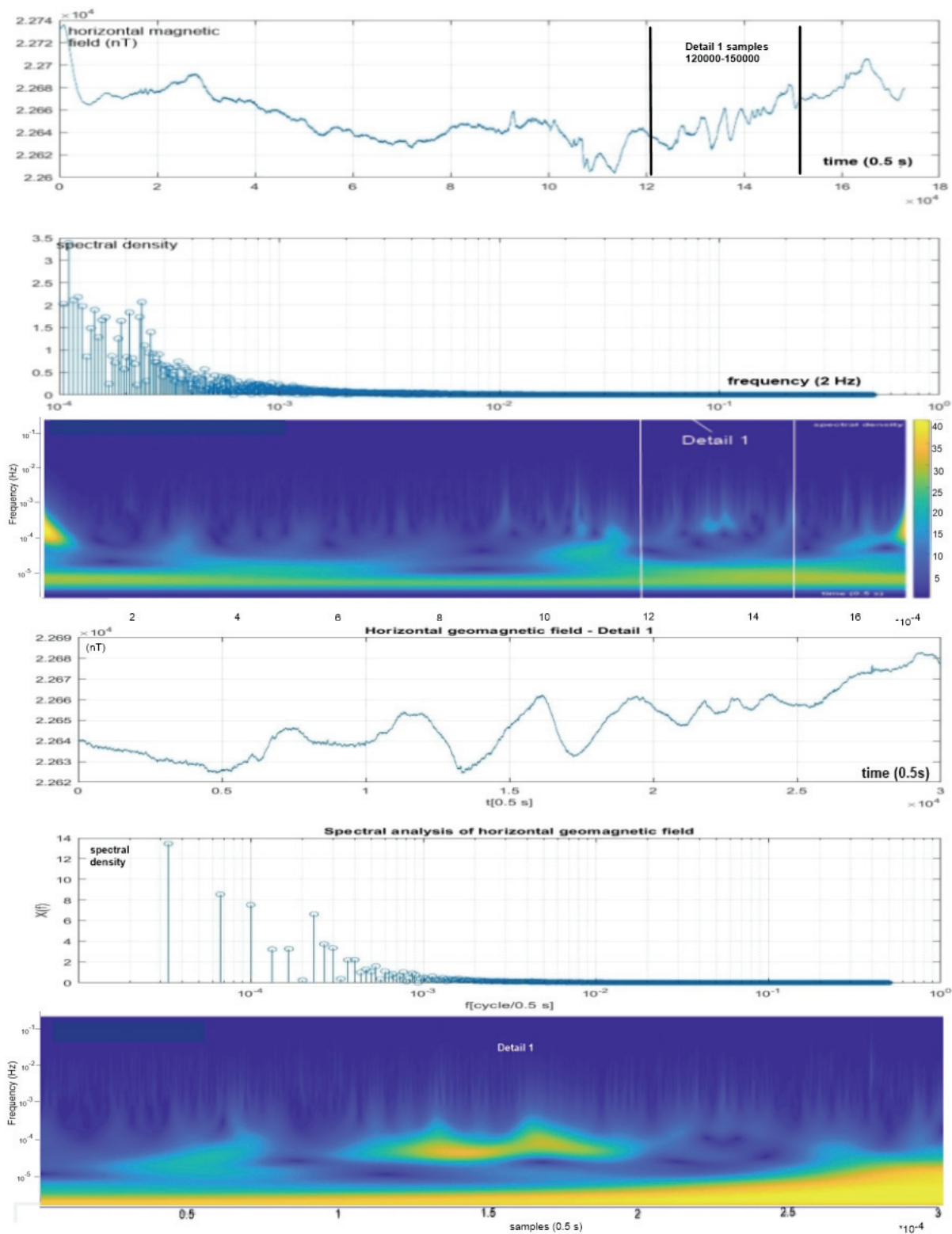


Figure 7. Time series, spectral analysis and wavelet analysis of horizontal geomagnetic field. From top to bottom the images have the following meaning: In the first three images we have the time series, Fourier analysis and wavelet analysis for all days of 2015, August 28, 00:00:00 to 24:00:00. In the last three images we have the time series, Fourier analysis and wavelet analysis for Detail 1 - interval 120000-150000 samples - a range of 4 hours and 10 minutes.

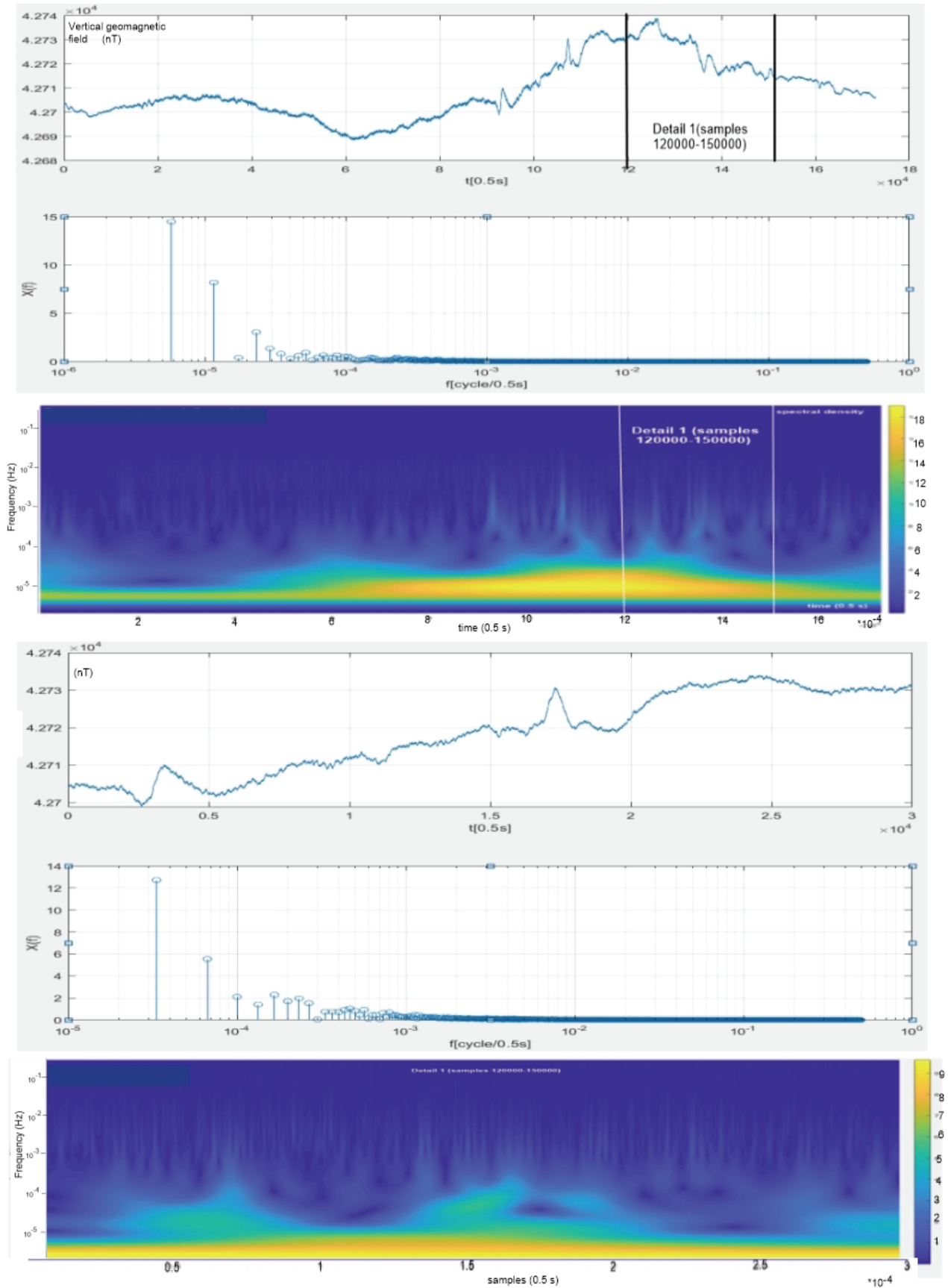


Figure 8. Time series, spectral analysis and wavelet analysis of vertical geomagnetic field. From top to bottom the images have the following meaning: In the first three images we have the time series, Fourier analysis and wavelet analysis for all days of 2015, August 28, 00:00:00 to 24:00:00. In the last three images we have the time series, Fourier analysis and wavelet analysis for Detail 1 - interval 120000-150000 samples - a range of 4 hours and 10 minutes.

In the Figs. 6, 7 and 8, there are similarities between the detail 1 and the corresponding portion of the full 24-hour signal. On the right sides of DWT images are the frequency scales found in the signal analysis.

The amplitude in the horizontal component (North magnetic direction) had variations of up to 120 nT, in the declination up to 25 minutes and in the vertical direction up to 50 nT. There is an increase in the number of frequencies between 1/500 Hz and 1/5000 Hz on all components, which corresponds to periods ranging from eight minutes to over one hour, belonging to the pulses of the categories pc5 (continuous pulses) and pi3 (irregular pulses). Associated with these pulses, we notice the overlapping of other higher frequencies with lower amplitude (from categories pc3, pc4 and pi2). These types of events reflect the geomagnetic activity specific to geomagnetic storms.

## CONCLUSIONS

A simple but effective way to highlight a geomagnetic storm is the calculation of gradients of geomagnetic components. Sudden geomagnetic variations (SSC, SI, SFE, geomagnetic storms) are relevant through Kp index (only for geomagnetic storms calculated for INTERMAGNET observatories).

The Kp indexes (6,4,4,3,5,5,6,4) from the site <https://www.spaceweatherlive.com/en/archive/2015/08/28/kp>, qualify the perturbations from August 28, 2015 in the category of M2 events, moderate storms and two sunspot regions on the disk. Solar wind speed, as measured by the ACE spacecraft, reached a peak speed of 440 km/s at August 28, 2015 and the maximum southward vertical component of magnetic field Bz reached 16 nT. Electrons greater than 2 MeV at geosynchronous orbit reached a peak level of 256 pfu. The statistical and spectral analysis of the geomagnetic field variation from geomagnetic observatories provides information on the geomagnetic pattern. In the wavelet charts, the frequencies are marked with colours between blue and yellow representing the weight of each frequency in the analysed signal. According with this, we can find the predominant frequency for each component at each time. The STFT tries to solve the problem in Fourier transform by introducing a sliding window  $w(t-u)$ . The detailed windows are designed to extract a small portions of the signal  $f(t)$  and then take Fourier transform. The transformed coefficient has two independent parameters. The wavelet functions are designed to strike a balance between time domain (finite length) and frequency domain (finite bandwidth).

As we dilate and translate the mother wavelet, we can see very low frequency components at large scale, while a very high frequency component can be located precisely at small scale.

## ACKNOWLEDGEMENT

We gratefully acknowledge the many and significant contributions and comments provided by our colleagues from geomagnetic observatories. The manual about observatories' methodologies is based on the original document (INTERMAGNET Technical Reference).

Also, we thank the support of the Ministry of Research for the funding of the project: "The realization of 3D geological / geophysical models for the characterization of some areas of economic and scientific interest in Romania", with Contract no. 28N / 2019 and project No. 16PCCDI/2018: "Institutional capacities and services for research, monitoring and forecasting of risks in extra-atmospheric space", within PNCDIII.

## REFERENCES

- ASIMOPOLOS N. S. & ASIMOPOLOS L. 2018. Study on the high-intensity geomagnetic storm from march 2015, based on terrestrial and satellite data, Micro and Nano Tehnologies & Space Tehnologies & Planetary Science. *Surveying Geology & Mining Ecology Management*. Conference Proceedings. **18**(6.1): 593-600.
- ASIMOPOLOS L., NICULICI E., SĂNDULESCU A. M., ASIMOPOLOS N. S. 2011. Comparisons of geomagnetic data measured in Romania with the data of International Geomagnetic Reference Field 11 (IGRF 11). *Surveying Geology & Mining Ecology Management*. Conference Proceedings **2**: 25-32.
- ASIMOPOLOS L., SĂNDULESCU A. M., ASIMOPOLOS N. S., NICULICI E. 2012. *Analysis of data from Surlari National Geomagnetic Observatory*. Edit. Ars Docendi. Universitatea București. 96 pp.
- BENOIT S. L. 2012. *INTERMAGNET Technical reference manual - Version 4.6*. British Geological Survey. Murchison House. Edinburgh. 100 pp.
- CHATFIELD C. 1989. *The Analysis of Time Series: An Introduction*. 4th Edit. Chapman and Hall. London. 241 pp.
- DAUBECHIES I. 1990. The wavelet transform time-frequency localization and signal analysis. *Institute of Electrical and Electronics Engineers. Transactions on Information Theory*. New York. **36**: 961-1004.
- GEBBINS D. & HERRERO-BERVERA E. 2007. *Encyclopedia of Geomagnetism and Paleomagnetism*. Springer. Berlin: 311-360.
- LIU C.-L. 2010. A tutorial of the wavelet transform (<http://disp.ee.ntu.edu.tw/tutorial/WaveletTutorial.pdf> (accessed January 20, 2019)).
- TORRENCE C. & COMPO G. P. 1998. A Practical Guide to Wavelet Analysis. *Bulletin of the American Meteorological Society*. Boston. **79**(1): 61-78.

- \*\*\*. International Real-time Magnetic Observatory Network. 2019. <http://www.intermagnet.org> (accessed February 01, 2019).
- \*\*\*. MathWorks. 2019. <https://www.mathworks.com> (accessed February 01, 2019).
- \*\*\*. National Oceanic and Atmospheric Administration. 2019. <http://www.noaa.gov> (accessed January 15, 2019).
- SpaceWeatherLive.com. 2019. <https://www.spaceweatherlive.com/en/archive/2015/08/28/kp> (accessed January 15, 2019).

## ANNEX

The code used for Fourier analysis in MATLAB:

```
load table.txt; X1= table (:,1); X2= table (:,2); X3= table (:,3); N=length(X1); t=1:1:N; fe=1/N; x=X1';
Xt=fft(x); Xm=abs(Xt); X=Xm(1,1:N/2+1)/(N/2); f=[0:N/2]*fe; subplot(211); plot(t,x); grid; xlabel('t[min]');
ylabel('x(t)[ ]'); title(' '); subplot(212); stem(f,X); xlabel('f[0.5Hz]'); ylabel('X(f)'); grid; title('')
```

The code used for wavelet analysis with function Daubechies db1, at level 5, in MATLAB:

```
load table.txt; SX=table(:,1); signal = SX; lev = 5; wname = 'db1'; nbc = 64; [c,l]
=wavedec(signal,lev,wname); len = length(signal); cfd = zeros(lev,len); for k = 1:lev; d = detcoef(c,l,k); d = d(:); d =
d(ones(1,2^k),:); cfd(k,:) = wkeep1(d(:),len); end
cfd = cfd(:); I = find(abs(cfd)<sqrt(eps)); cfd(I) = zeros(size(I)); cfd = reshape(cfd,lev,len); cfd =
wcodemat(cfd,nbc,'row'); h211 = subplot(2,1,1); h211.XTick = []; plot(signal,'r'); title('Analyzed signal. '); ax = gca;
ax.XLim = [1 length(signal)]; subplot(2,1,2); colormap(cool(128)); image(cfd); tics = 1:lev; labs = int2str(tics); ax =
gca; ax.YTickLabelMode = 'manual'; ax.YDir = 'normal'; ax.Box = 'On'; ax.YTick = tics; ax.YTickLabel = labs;
title('Discrete Transform, absolute coefficients. '); ylabel('Level'); figure; [cfs,f] = cwt(signal,1,'waveletparameters',[3
3.1]); hp = pcolor(1:length(signal),f,abs(cfs)); hp.EdgeColor = 'none'; set(gca,'YScale','log'); xlabel('Sample');
ylabel('log10(f)').
```

### Asimopolos Laurențiu

Geological Institute of Romania  
1st Caransebeș Street, 012271 - Bucharest, Romania.  
E-mails: laurentiu.asimopolos@igr.ro, asimopolos@gmail.com

### Asimopolos Adrian Aristide

University POLITEHNICA of Bucharest  
Faculty of Transports, 313 Splaiul Independentei, 060042 - Bucharest, Romania.  
E-mail: adrian.asimopolos@gmail.com

### Asimopolos Natalia-Silvia

Geological Institute of Romania  
1st Caransebeș Street, 012271 - Bucharest, Romania.  
E-mails: natalia.asimopolos@igr.ro, asi\_nata@yahoo.com

Received: February 12, 2019

Accepted: July 22, 2019